

blood

2012 120: 2708-2718
Prepublished online August 16, 2012;
doi:10.1182/blood-2012-04-422337

Dysmegakaryopoiesis of FPD/AML pedigrees with constitutional *RUNX1* mutations is linked to myosin II deregulated expression

Dominique Bluteau, Ana C. Glembotsky, Anna Raimbault, Nathalie Balayn, Laure Gilles, Philippe Rameau, Paquita Nurden, Marie Christine Alessi, Najet Debili, William Vainchenker, Paula G. Heller, Remi Favier and Hana Raslova

Updated information and services can be found at:
<http://bloodjournal.hematologylibrary.org/content/120/13/2708.full.html>

Articles on similar topics can be found in the following Blood collections
[Platelets and Thrombopoiesis](#) (302 articles)

Information about reproducing this article in parts or in its entirety may be found online at:
http://bloodjournal.hematologylibrary.org/site/misc/rights.xhtml#repub_requests

Information about ordering reprints may be found online at:
<http://bloodjournal.hematologylibrary.org/site/misc/rights.xhtml#reprints>

Information about subscriptions and ASH membership may be found online at:
<http://bloodjournal.hematologylibrary.org/site/subscriptions/index.xhtml>



Dysmegakaryopoiesis of FPD/AML pedigrees with constitutional *RUNX1* mutations is linked to myosin II deregulated expression

Dominique Bluteau,^{1,3} Ana C. Glembotsky,⁴ Anna Raimbault,^{1,3} Nathalie Balayn,^{1,3} Laure Gilles,^{1,3} Philippe Rameau,² Paquita Nurden,⁵ Marie Christine Alessi,⁶ Najet Debili,^{1,3} William Vainchenker,^{1,3} Paula G. Heller,⁴ *Remi Favier,^{1,5,7} and *Hana Raslova^{1,3}

¹Institut National de la Santé et de la Recherche Médicale, Villejuif, France; ²Institut Gustave Roussy, Villejuif, France; ³Université Paris Sud, Villejuif, France; ⁴Instituto de Investigaciones Médicas Alfredo Lanari, Universidad de Buenos Aires, Consejo Nacional de Investigaciones Científicas y Técnicas, Buenos Aires, Argentina; ⁵Centre de Référence des Pathologies Plaquettaires, Hôpital Haut-Lévêque, Pessac, France; ⁶Institut National de la Santé et de la Recherche Médicale, Faculté de Médecine La Timone, Marseille, France; and ⁷Assistance Publique-Hôpitaux de Paris, Hôpital Trousseau, Service d'Hématologie biologique, Paris, France

FPD/AML is a familial platelet disorder characterized by platelet defects, predisposition to acute myelogenous leukemia (AML) and germ-line heterozygous *RUNX1* alterations. Here we studied the in vitro megakaryopoiesis of 3 FPD/AML pedigrees. A 60% to 80% decrease in the output of megakaryocytes (MKs) from CD34⁺ was observed. MK ploidy level was low and mature MKs displayed a major defect in proplatelet formation. To

explain these defects, we focused on myosin II expression as *RUNX1* has been shown to regulate MYL9 and MYH10 in an inverse way. In FPD/AML MKs, expression of MYL9 and MYH9 was decreased, whereas MYH10 expression was increased and the MYH10 protein was still present in the cytoplasm of mature MKs. Myosin II activity inhibition by blebbistatin rescued the ploidy defect of FPD/AML MKs. Finally, we demonstrate that MYH9

is a direct target of *RUNX1* by chromatin immunoprecipitation and luciferase assays and we identified new *RUNX1* binding sites in the *MYL9* promoter region. Together, these results demonstrate that the defects in megakaryopoiesis observed in FPD/AML are, in part, related to a deregulation of myosin IIA and IIB expression leading to both a defect in ploidization and proplatelet formation. (*Blood*. 2012;120(13):2708-2718)

Introduction

Familial platelet disorder with predisposition to acute myeloid leukemia (FPD/AML, OMIM 601399) is an autosomal dominant disorder characterized by dysmegakaryopoiesis, qualitative and quantitative platelet defects, and a propensity to develop myelodysplastic syndromes (MDSs) and/or AML. Several types of heterozygous germ-line mutations or deletions in *RUNX1*, including missense, frameshift, and nonsense mutations or large intragenic deletion or single nucleotide deletion in the Runt domain have been identified in FPD/AML. The progression to AML is often linked to the somatic alteration of the second *RUNX1* allele,¹ supporting the fact that *RUNX1* acts as a tumor suppressor gene. *RUNX1* (also known as AML1, PEBP2aB, or CBFa2) is 1 of the 3 DNA-binding α subunits of the hematopoietic transcription complex called core binding factor (CBF). *RUNX1* contains both a runt homology domain (RHD), which mediates DNA binding and heterodimerization with the core binding factor β (CBF β) subunit to stabilize the interaction of the complex with DNA and to protect CBF from proteolytic degradation. The C-terminal domain of *RUNX1* is responsible for transcriptional activation. *RUNX1* can act as a repressor or an activator depending on the cellular context. It regulates positively different hematopoietic genes encoding cytokines and their receptors, such as IL-3,² GM-CSF, and M-CSF or negatively the CD4 gene contributing thus to impaired T-cell development.³ Somatic alterations in *RUNX1* are frequently found in AML, MDS, and chronic myelomonocytic leukemia (CMML).

In different mouse models, *RUNX1* was shown to be essential for establishing definitive hematopoiesis.⁴ It is required for the generation of hematopoietic stem cells (HSCs) from the aorta, but not later on. Targeted deletion of *RUNX1* in adult HSCs led to their expansion in bone marrow, but also to amplification of progenitor cells with altered self-renewal capacities, which might be the first event toward leukemic transformation. The increased clonogenic potential and some self-renewal capacities of immature hematopoietic progenitors were also described for FPD/AML patients and were correlated with an almost complete loss in expression of the *RUNX1* target NR4A3.⁵ *RUNX1* is dispensable for HSC commitment to myeloid lineages and to double-negative CD4/CD8 thymocytes, but is essential for terminal differentiation of the MK and T-lymphoid lineages. Especially, its absence profoundly affects MK polyploidization and terminal maturation resulting in thrombocytopenia.⁶⁻⁸ In human, heterozygous germ-line *RUNX1* mutations found in FPD/AML lead to diminished number of CFU-MK in bone marrow with abnormally small size MK.⁹

Deregulation of a large number of genes associated with microtubules and cytoskeleton structures that could be involved in platelet formation was detected in EBV cell lines obtained from FPD/AML patients and in cell lines overexpressing the CBF complex.¹⁰ In addition, patient's platelets abnormally express several proteins, such as protein kinase C θ (PKC- θ), platelet type 12-lipoxygenase (12-LO), myosin light chain, and others.¹¹

Submitted April 5, 2012; accepted July 24, 2012. Prepublished online as *Blood* First Edition paper, August 16, 2012; DOI 10.1182/blood-2012-04-422337.

*R.F. and H.R. contributed equally to this work.

The online version of this article contains a data supplement.

The publication costs of this article were defrayed in part by page charge payment. Therefore, and solely to indicate this fact, this article is hereby marked "advertisement" in accordance with 18 USC section 1734.

© 2012 by The American Society of Hematology

However, the precise mechanisms by which RUNX1 regulates megakaryopoiesis, platelet formation and functions are not completely understood. Among direct RUNX1 target genes implicated in megakaryopoiesis and platelet functions, the thrombopoietin (TPO) receptor MPL has the best-characterized function. MPL is regulated negatively in HSCs and positively in MKs by RUNX1. Consistent with these results, MPL mRNA level in platelets of 1 FPD/AML pedigree was shown to be decreased.¹² However, a partial defect in MPL expression might lead to thrombocytosis rather than to thrombocytopenia as revealed in a mouse model,¹³ suggesting that deregulation of other proteins might be involved in FPD/AML thrombocytopenia. P19^{INK4D}, a second RUNX1 target, plays an important role in the cell-cycle arrest in MKs and regulates ploidy.¹⁴ However, in vivo p19^{INK4D} defect leads to normal or increased platelet counts. A negative regulator of megakaryopoiesis PF4¹⁵ is also a direct RUNX1 target¹⁶ and its level is decreased in platelets of FPD/AML patients.¹¹ Other genes regulated by RUNX1 may be more implicated in platelet functions. The promoters of α IIb and α 2 integrins are activated by RUNX1 in cooperation with GATA1 in K562 cells.¹⁷ 12-lipoxygenase, a direct RUNX1 target,¹⁸ regulates GPIIb-GPIIIa activation and platelet aggregation after adenosine diphosphate (ADP), thrombin or U46619 stimulation.^{19,20} MYL9 is deeply decreased in platelets of FPD/AML patients and is a direct target of RUNX1 in the HEL cell line.²¹ Moreover, we recently demonstrated that RUNX1 negatively regulates nonmuscle myosin heavy chain (NMMHC-IIb, MYH10) and that MYH10 silencing is necessary to the switch from mitosis to endomitosis.²²

To get insight into the regulation of megakaryopoiesis by RUNX1, we investigated the in vitro megakaryopoiesis derived from CD34⁺ hematopoietic progenitors of 3 FPD/AML pedigrees, one harboring the R174Q mutation, another harboring the R139X mutation⁵ and the last a Pro218fsX225,¹² but renamed as T219RfsX8 according to current mutation nomenclature (www.hgvs.org/mutnomen). In parallel, we studied the effect of RUNX1 knock-down in normal MKs. By both approaches, we demonstrated that RUNX1 controls at least partially MK ploidization and proplatelet formation by a direct regulation of MYL9, MYH10, and MYH9.

Methods

Blood samples

Blood samples from FPD/AML patients, healthy subjects, and individuals after mobilization were collected after informed written consent was obtained in accordance with the Declaration of Helsinki. The study was approved by the Local Research Ethic Committee from the Assistance Publique-Hôpitaux de Paris (AP-HP).

In vitro growth of megakaryocytes from CD34⁺ cells

Patient or control CD34⁺ cells were isolated using an immunomagnetic bead technique (Miltenyi Biotec)²³ and grown in serum free medium as previously reported.²⁴ The medium was supplemented with a cytokine cocktail containing TPO (10 ng/mL; Kirin Brewery), interleukin-3 (IL-3; 100 U/mL; Novartis), Interleukin-6 (IL-6; 10 ng/mL; Tebu), stem cell factor (SCF; 25 ng/mL, Biovitrum AB), and fetal liver tyrosine kinase 3 ligand (FLT3-L; 1 ng/mL, Celldex Therapeutics).

Flow cytometry analysis

Cells were stained with directly coupled MoAbs: anti-CD41 APC and anti-CD42 PE (BD Bioscience) for 30 minutes at 4°C. Depending on the experiments, MKs were sorted according to CD41 or CD41 and CD42

expression using an influx flow cytometer equipped with 5 lasers (BD Bioscience).

Cell transduction

Control CD34⁺ cells (10⁶/mL) were prestimulated for 24 hours with TPO, IL-3, SCF, and FLT3-L. Lentiviral particles were then added at a concentration corresponding to 125 ng viral p24/100 μ L for 12 hours, followed by a second transduction. Cells were then cultured in the presence of TPO alone. Lentivirus vectors containing shRUNX1_1 or a control scramble sequence (control) in addition to the sequence encoding GFP were previously described.¹⁴ Another shRUNX1_2 sequence (5'-ggcagaaactagatgatca-3') was also cloned into the sinPRRL-PGK-GFP lentivirus. Virus particles production and cell transduction were performed as previously described.¹⁴

Ploidy analysis

At day 6 of culture, blebbistatin (25 μ M) diluted in DMSO or DMSO alone was added to the culture. Seventy-two hours later, Hoechst 33342 (10 μ g/mL; Sigma-Aldrich) was added in the medium of cultured MKs for 2 hours at 37°C. Cells were then stained with directly coupled mAbs: anti-CD41 APCs, and anti-CD42 PE (BD Bioscience) for 30 minutes at 4°C.²⁵ Ploidy was measured in the CD41⁺CD42⁺ cell population by an influx flow cytometer (BD Bioscience). The mean ploidy of human MKs was calculated by the following formula: (2N \times the number of cells at 2N ploidy level + 4N \times the number of cells at 4N ploidy level + ... + 64N \times the number of cells at 64N ploidy level/the total number of cells).

Quantification of MKs bearing proplatelets

Lentivirus transduced GFP⁺CD41⁺CD42⁺ MKs from healthy donors or CD41⁺CD42⁺ MKs from patients were sorted at day 9 of culture and plated in 96-well plates at a concentration of 2000 cells/well in serum-free medium in the presence of TPO (10 ng/mL). Four days later, MKs displaying proplatelets were quantified by enumerating 500 cells/well using an inverted microscope (Carl Zeiss) at a magnification of \times 200. MKs displaying proplatelets were defined as cells exhibiting 1 or more cytoplasmic processes with constriction areas (3 wells were examined for each condition). Images were obtained using AxioVision 4.6 software.

Quantitative real-time PCR

mRNA isolation, reverse transcription and real-time PCR (RT-PCR) analyses were performed as described.¹⁴ The expression levels of all genes studied were expressed relatively to housekeeping genes PPIA and HPRT with stable expression level during MK differentiation. Primer sequences are available on request.

ChIP and promoter activity assays

Chromatin immunoprecipitation (ChIP) assays were performed with a ChIP assay kit (Millipore Upstate Biotechnology) using the anti-RUNX1 antibody (8 μ g per sample, sc-65; Santa Cruz Biotechnology). Assays were performed using chromatin prepared from human MKs as previously described.¹⁴ Immunoprecipitated DNA was analyzed on a PRISM 7700 sequence detection system using SYBR green (Applied Biosystems) in duplicate. Two independent experiments were performed. Primer sequences are available on request.

Luciferase reporter assay

HEL cells were cotransfected with the reporter plasmids plucMYL9 or plucMYH9 without or with mutation in the RUNX1 binding site (plucMYL9mut1, mut2 or mut1/2, and plucMYH9mut1) and with TK-Renilla reporter (Promega) for normalization of transfection efficiency. Cells were harvested 48 hours after transfection. A dual luciferase assay was performed according to the manufacturer's instructions (Promega). The luciferase activity was measured with an AutoLumat LB953 luminometer (Berthold).

Immunofluorescence and cytologic study

Immunofluorescence was performed on cells at day 10 of culture. Cells were seeded on polylysine coated slides (CML) for 2 hours at 37°C (5% CO₂ in air). After a gentle wash, adherent cells were fixed in 2% paraformaldehyde for 10 minutes, permeabilized with 0.1% Triton X-100 for 5 minutes and washed with 1× PBS for 5 minutes. Primary antibodies were subsequently applied to the slides at a concentration of 1 µg/mL and incubated for 1 hour at room temperature. Slides were then washed 3 times with 1× PBS for 5 minutes before and after application of the secondary antibody (20 µg/mL) for 30 minutes at room temperature. Finally, slides were mounted using either Vectashield with Dapi (Molecular Probes) and examined under a Leica DMI 4000, SPE, laser scanning microscope (Leica Microsystem) with a 63×/1.4 numeric aperture (NA) oil objective. Images were processed using Adobe Photoshop 6.0 software. Twenty MKs positive for von Willebrand factor (VWF) were analyzed for each individual. The following antibodies were used: rabbit anti-MYH10 (Cell Signaling), rabbit anti-MYH9 (Cell Signaling), and mouse anti-VWF. Appropriate secondary antibodies were conjugated with Alexa 488 or Alexa 546 (Molecular Probes).

Bone marrow smears were stained by the May-Grünwald-Giemsa technique.

Electron microscopy

Venous blood was taken in ACD-A (1 vol/7 vol) and centrifuged for 10 minutes at 170g. Platelet-Rich Plasma (PRP) was carefully aspirated and incubated for 20 minutes at 37°C. Platelets were fixed in 1.25% glutaraldehyde (Fluka Chemie) and diluted in 0.1 M phosphate buffer (pH 7.2) for 1 hour at room temperature. For morphometry, a minimum of 100 sections was analyzed for each subject; platelet diameters and surface area were measured using ImageJ 1.46r (National Institutes of Health). Samples were processed for EM by standard procedures previously described.²⁶ Sections were observed with a Jeol JEM-1010 transmission electron microscope (Jeol) at 80 kV.

Statistical analyses

Data are presented as means ± SD. Statistical significance was determined by Student *t* test. A *P* value < .05 was considered as statistically significant.

Results

Defect in megakaryocyte differentiation and polyploidization in FPD/AML

The in vitro megakaryopoiesis of 2 patients in 3 different FPD/AML pedigrees was studied: AII-1 and AII-2 from the first pedigree (R174Q mutation),⁵ BII-2 and BII-3 from the second pedigree (R139X mutation),⁵ and DIII-1 and DIII-3 from the third pedigree (T219RfsX8 mutation)¹² (supplemental Table 1, available on the Blood Web site; see the Supplemental Materials link at the top of the online article). As we confirmed in 2 other FPD/AML patients who MPL expression was down-regulated,¹² peripheral blood CD34⁺ cells were grown in liquid medium in the presence of a combination of cytokines (IL-3, IL-6, FLT3-L, SCF, and TPO). At day 10, MKs were analyzed on the expression of CD41 and CD42. In patient cultures from the 3 pedigrees, the percentage of mature CD41⁺CD42⁺ MKs was decreased in comparison to the controls. A profound decrease was observed for the 3 pedigrees: from 12% for control to 1.6% for AII-1 and 1.01% for AII-2 patients; from 60% for control to 8.7% for BII-2 and 9.15% for BII-3 patients and from 25% for control to 1.26% for DIII-1 and 6.53% for DIII-3 patients (*n* = 3 for controls [32.33 ± 22.21] and *n* = 6 for patients [4.7 ± 3.8], *P* < .05; Figure 1A). When the total number of MKs produced in culture after 10 days was calculated, a moderate 3.55 ± 0.75-fold decrease in MK number was observed in pedigree

A (from 321 × 10³ MKs to 114 × 10³ MKs for AII-1 and 73 × 10³ MKs for AII-2 patients) whereas an important 15.5 ± 2.8-fold and 29.4 ± 0.95-fold decrease was seen, respectively in the pedigree B and D. When MKs were cultured from CD34⁺ progenitors of pedigree B patients, the absolute MK number was 903 × 10³ for control and only 71 × 10³ and 49 × 10³ for patients BII-2 and BII-3, respectively. Finally, in the study of pedigree D, 136 × 10³ MKs were generated in vitro for control and only 4.4 × 10³ and 4.1 × 10³ MKs for DIII-1 and DIII-3 patients (*n* = 3 for controls [453.3 × 10³ ± 231.1 × 10³] and *n* = 6 for patients [52.5 × 10³ ± 17.5 × 10³], *P* < .05; Figure 1B). This indicated not only a blockage in MK maturation but also an important decrease in the number of MK progenitors and/or in their proliferation.

Polyploidization is an important step of MK maturation as MK amplify their DNA content and cytoplasmic volume before proplatelet formation and platelet production. Ploidy level is markedly decreased in murine *runx1* KO MK^{6,7,22} and shRNA-mediated RUNX1 knockdown in human CD34⁺ cells leads to a decrease in MK ploidy level.²² We therefore investigated the ploidy of MKs from the 6 FPD/AML patients. Although in our culture conditions MKs did not reach a high ploidy, for all patients the MK ploidy level was significantly decreased compared with controls: from 3.4N to 2.8N and 2.9N in pedigree A, from 3.5N to 2.2N and 2.6N in pedigree 2 and from 3.6N to 2.6N and 2.8N in pedigree 3 [*n* = 3 for controls (3.5 ± 0.057N) and *n* = 6 for patients (2.65 ± 0.1N), *P* < .001] (Figure 1C). To confirm these results in the in vivo situation, we performed cytologic investigations of the bone marrow from 3 FPD/AML patients. We could detect the presence of numerous atypical MKs including immature MKs with high nucleocytoplasmic ratio and poorly lobulated nuclei (patients AII-1, DIII-3) associated with microMKs (patient BII-2; Figure 1D). The number of these abnormal MKs was increased in all patients. Altogether these results indicate that FPD/AML is associated with a decreased MK ploidy both in vitro and in vivo.

Proplatelet formation is profoundly altered in FPD/AML pedigrees

To further analyze the late stages of MK differentiation in patient samples, we studied the proplatelet formation. To this aim, CD41^{high}CD42^{high} mature MKs were sorted from cultures at day 9 and seeded in 96-well plates at 2 × 10³ cells per well in presence of TPO alone. Proplatelet formation was analyzed 4 days later (at day 13 of culture). The percentage of proplatelet-forming MKs was 20-fold reduced for AII-1 and AII-2 patients (R174Q) and 5-fold for BII-2 and BII-3 patients (R139X) in comparison with control proplatelet-forming MKs (Figure 2A-B, 3 independent experiments were performed for each patient, *n* = 3, *P* < .05).

Electron microscopy of blood platelets from patient AII-1 and BII-2 revealed numerous abnormalities including marked size heterogeneity with the presence of very large round platelets and others extremely thin. Incompletely fragmented proplatelet-like structures were also present. Figure 2C illustrates the presence of 2 joined platelets (designated as proplatelets, patient AII-1) and a succession of joined platelets (designated as unseparated proplatelets, patient BII-2). Such structures were often seen on low power magnification of enlarged fields. This incomplete fragmentation could be because of a defect in actin-myosin contractility or microtubule reorganization during the formation of cleavage furrow before fission event. Large vacuoles and giant granules also characterized platelets of both patients. Overall, these observations (Figure 2C) suggest an altered megakaryopoiesis and a defect in

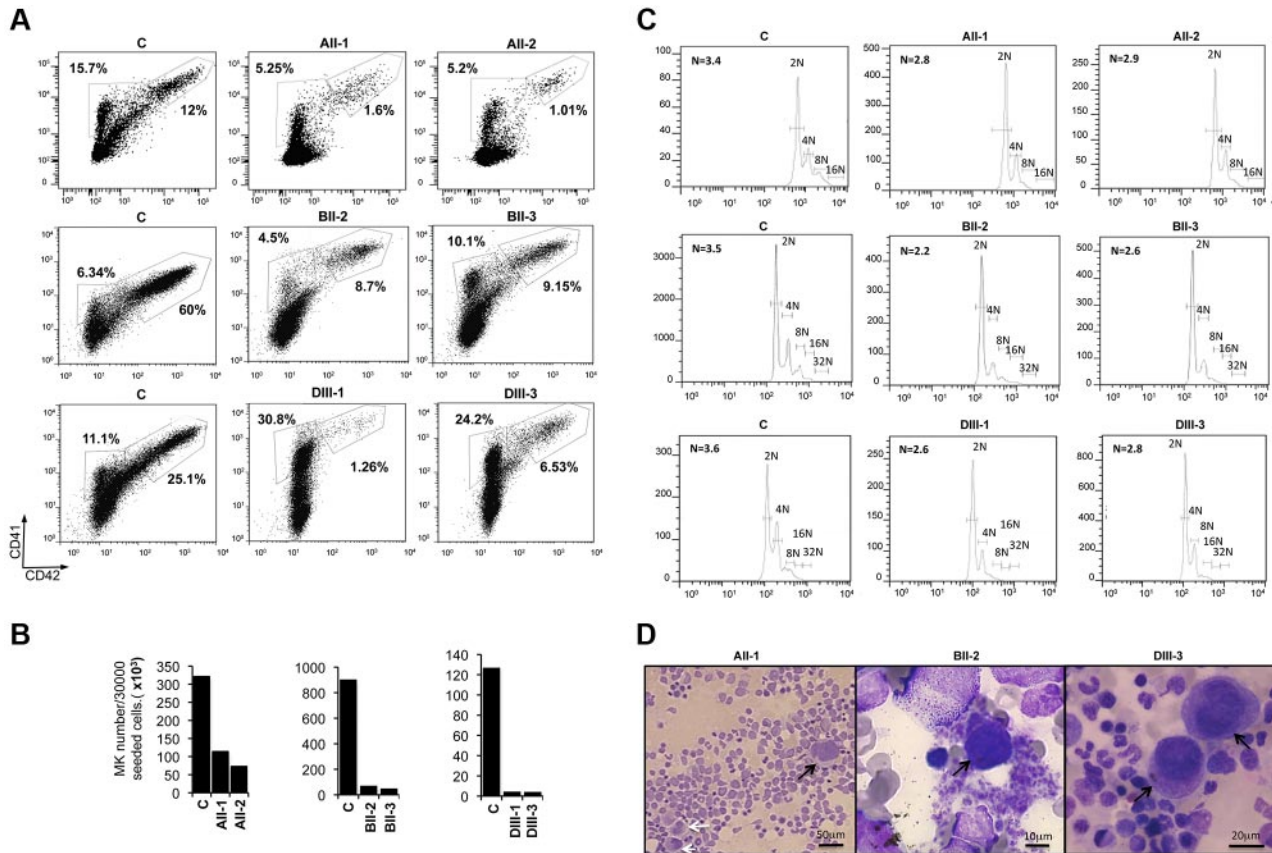


Figure 1. Assessment of in vitro MK differentiation from control and FPD/AML patient CD34⁺ cells. CD34⁺ peripheral blood cells from AII-1, AII-2, BII-2, BII-3, DIII-1, and DIII-3 patients and from 3 healthy individuals (C) were grown in liquid medium containing TPO, IL-3, IL-6, SCF, and FLT3-L. (A-C) One experiment was performed for each patient; the results obtained for all 6 patients were used for the calculation of statistics. (A) Flow cytometry analysis was performed at day 10 of culture. Percentage indicates the proportion of immature (CD41⁺CD42⁻) and mature (CD41⁺CD42⁺) MKs ($n = 3$ for controls and $n = 6$ for patients, $P < .05$). (B) Absolute number of MKs was calculated at day 10 of culture. The calculation was based on the total cell number at day 1 and day 10 of culture, and on the percentage of mature (CD41⁺CD42⁺) MKs (A). As the number of cells seeded at the day 1 was not identical, the absolute number was estimated per 3×10^4 seeded CD34⁺ cells ($n = 3$ for controls and $n = 6$ for patients, $P < .05$). (C) The ploidy of mature (CD41⁺CD42⁺) MKs was analyzed for 3 controls and 6 patients at day 10 of culture ($n = 3$ for controls and $n = 6$ for patients, $P < .001$). (D) Cytologic investigations of the bone marrow of AII-1, BII-2, and DIII-3 patients. The numerous atypical hypolobulated MKs (black arrows) and microMKs (white arrows) are present.

proplatelet fragmentation. A morphometric quantitative analysis of platelet shows that the small diameter remained close to the normal range but the large diameter is decreased (BII-2, supplemental Table 2). Many of the platelets have a tendency to be round as confirmed by the increase in the percentage of platelets with a maximal/minimal diameter ratio < 2 .

RUNX1 knockdown also leads to a defect in MK differentiation and proplatelet formation

To test the effect of RUNX1 knockdown on MK differentiation, we used 2 different RUNX1 shRNA (supplemental Figure 1A-B). We performed liquid cultures and studied the percentage of CD41 and CD42 positive cells at day 9. Compared with CD34⁺ cells transduced with a scramble shRNA (control), a 2-fold decrease in the percentage of mature CD41^{high}CD42^{high} MKs was detected using shRUNX1_1 ($n = 3$, $P < .05$, Figure 3B) or shRUNX1_2 (data not shown). This was really a defect in MK maturation as expression of both GPIIB (CD41), which may be regulated by RUNX1¹⁷ and GPIB (CD42) were decreased. This result demonstrates that RUNX1 knockdown affects MK differentiation (Figure 3A).

To investigate proplatelet formation, MK transduced by the scramble shRNA (control) or shRUNX1_1 or shRUNX1_2 were cultured in medium containing TPO alone. CD41^{high}CD42^{high}GFP⁺ MKs were sorted at day 9 and seeded in 96-well plates at 2×10^3 cells

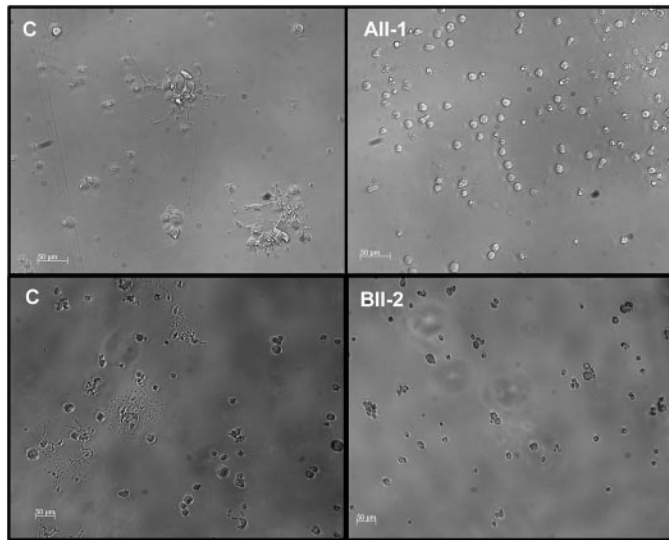
per well in presence of TPO alone and analyzed 4 days later. A significant 1.6-fold decrease in the percentage of proplatelet-forming MKs was observed with shRUNX1_1 whereas, shRUNX1_2 elicited an even more profound decrease (more than 5-fold; $n = 3$, $P < .05$, Figure 3B-C). This result parallels the effects of the 2 shRNA on RUNX1 expression (supplemental Figure 1B).

Thus, the phenotype of FPD/AML and RUNX1 knockdown MKs was similar with a defect in maturation and proplatelet formation as well as in ploidy.²²

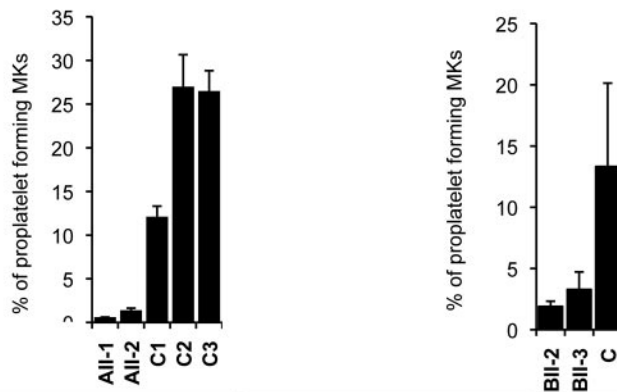
A defect in myosin II expression defect is present in FPD/AML megakaryocytes

Nonmuscle myosins II play an important role in MK differentiation with myosin IIB involved in cytokinesis and ploidy, and myosin IIA in migration and proplatelet formation.^{22,27,28} There is already evidence that RUNX1 directly regulates MYL9, the myosin light chain and MYH10, the myosin IIB heavy chain, in an inverse way. All these observations led us to hypothesize that a deregulated expression of myosin II isoforms might be present in FPD/AML MKs and might thus participate in the thrombocytopenia mechanism. During normal MK differentiation, MYH9 expression increases, whereas MYH10 decreases.²² However, whether changes in myosin light chain (MLC) expression occurs during

A



B



C

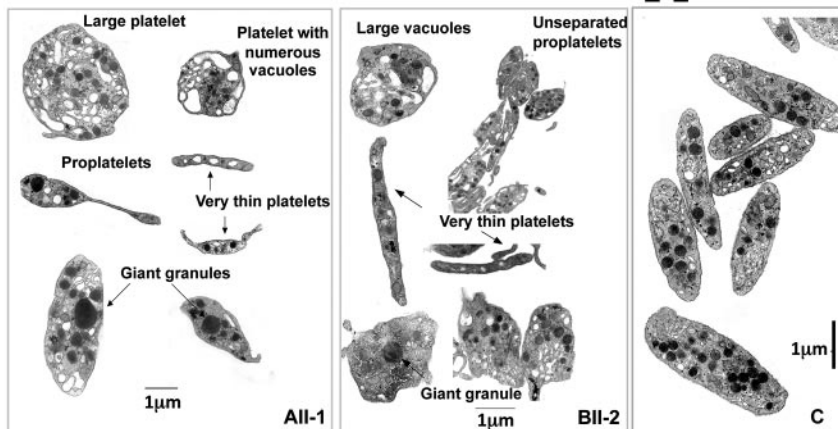


Figure 2. Effect of *RUNX1* mutations on MK differentiation and proplatelet formation. (A-B) CD34⁺ cells from AII-1, AII-2, BII-2, and BII-3 patients and control individuals were grown in liquid medium supplemented with TPO, IL-3, IL-6, SCF, and FLT3-L. C1, C2, and C3 were grown simultaneously with AII-1 and AII-2, and C was grown simultaneously with BII-2 and BII-3. CD41⁺CD42⁺ cells were sorted at day 10 of culture and seeded at 2×10^3 cells/well in 96-well plate. The percentage of proplatelet forming MKs was estimated at day 13. (A) Representative microscopic images representing control and patients proplatelet forming MKs. (B) The percentage of proplatelet forming MKs was estimated by counting MKs exhibiting 1 or more cytoplasmic processes with areas of constriction. A total of 500 cells per well was counted. The histograms show 1 representative experiment of 3, each in triplicate. Error bars represent \pm SD of triplicate ($n = 3$, $P < .05$). (C) Ultrastructural aspect of blood platelets from AII-1 and BII-2 patients. Gallery of photographs illustrating the typical platelet abnormalities: large heterogeneity in size with both round enlarged and small thin platelets, presence of giant granules and large vacuoles, presence of incompletely fragmented proplatelets. Similar results were obtained in 3 repeated experiments.

MK differentiation is unknown. We thus investigated the mRNA expression levels of the 4 MLCs, namely MYL12A, MYL12B, MYL9, and MYL6. To this purpose, CD41⁺ cells were sorted at day 6, cultured in presence of SCF and TPO, and analyzed at days 6, 9, and 14. As shown in Figure 4A, mRNA levels of all MLCs increased along MK differentiation. Notably, at terminal stages of MK differentiation, mRNA expression level of MYL12A was approximately 7-fold higher than the other MYL (D14, Figure 4A).

Next, we investigated the expression of *MYL* and *MYH* genes at mRNA level in mature CD41^{high}CD42^{high} MKs of 6 FPD/AML patients and 4 healthy subjects. We first confirmed a profound decrease in MYL9 mRNA level in patient's MKs compared with controls ($P < .01$); in addition, MYH9 transcripts were also

significantly decreased (50%, $P < .05$), whereas MYH10 transcripts were significantly increased ($P < .05$); no change in MYL12A and MYL12B expression was seen between patients and controls (Figure 4B). However, even when MYH9 was decreased and MYH10 was increased, MYH9 remained the predominant myosin heavy chain in FPD/AML MK as a consequence of the very high MYH9 expression level in MKs (Figure 4C). As *RUNX1* is involved in the silencing of MYH10 in mature MKs, we investigated whether MYH10 protein could be detected in mature MKs of FPD/AML. Using immunofluorescence staining, MYH10 was present in mature MKs from all FPD/AML patients (Figure 4D; for BII-2, DIII-1, and DIII-3 patients) in contrast to normal MKs. Moreover, MYH10 localization was diffuse in the cytoplasm and

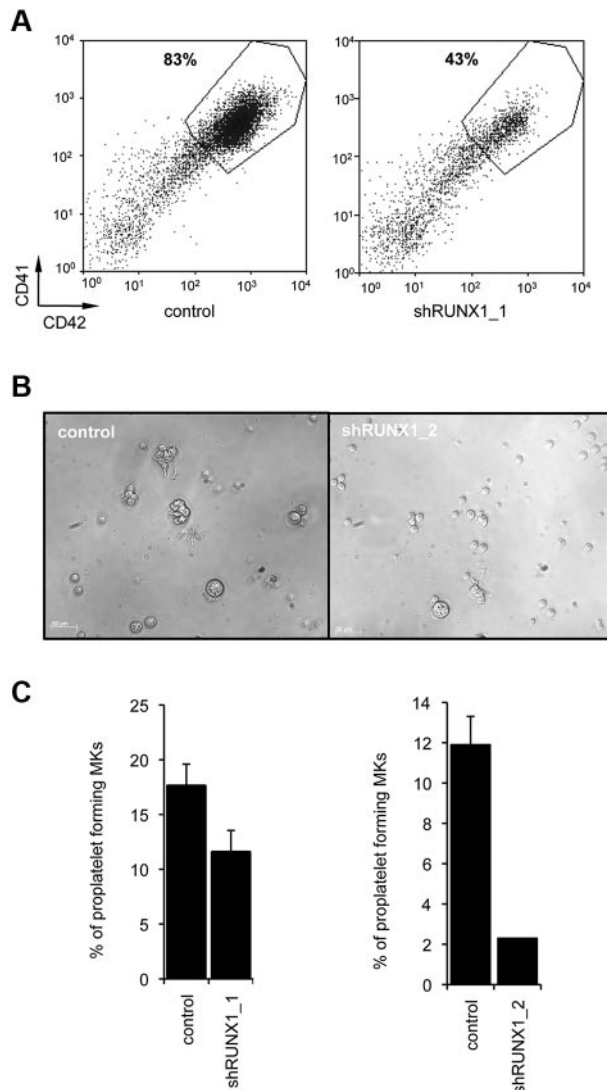


Figure 3. Effect of RUNX1 knockdown on in vitro megakaryopoiesis. CD34⁺ cells from control individuals were transduced with a lentivirus encoding either scramble shRNA (control) or RUNX1_1 shRNA or RUNX1_2 shRNA. Transduced CD34⁺ cells were grown in liquid medium in presence of TPO, IL3, IL6, SCF, and FLT3-L. (A) Flow cytometry analysis was performed after 10 days of culture. A representative analysis of 3 repeated experiments is shown. (B-C) CD41⁺CD42⁺GFP⁺ cells were sorted at day 10 of culture and seeded at 2×10^3 cells/well in 96-well plates. The percentage of proplatelet-forming MKs was estimated at day 13. (B) Representative microscopic images representing control and shRUNX1_2 transduced proplatelet-forming MKs. (C) The percentage of proplatelet-forming MKs was estimated by counting MKs exhibiting 1 or more cytoplasmic processes with areas of constriction. A total of 500 cells per well was counted. The histograms show 1 representative experiment of 3, each in triplicate. Error bars represent \pm SD of triplicate ($n = 3$ for both shRUNX1_1 and shRUNX1_2, $P < .05$).

did not concentrate at the membrane oppositely to MYH9. These results show that MYH9 and MYH10 have different localizations and thus may have different functions.

MYL9 and MYH9 are both direct RUNX1 targets in primary megakaryocytes

Next, we explored the molecular mechanisms underlying the ability of RUNX1 to regulate MYL9 and MYH9. To address whether MYL9 and MYH9 were direct transcriptional targets of RUNX1, we performed an in silico sequence analysis²⁹ of the MYL9 and MYH9 promoter region 1Kb upstream the transcription start site. In the MYL9 promoter, we identified a novel region

different from the one already described²¹ containing potential RUNX1 binding sites and 2 potential RUNX1 binding sites in the MYH9 promoter (supplemental Table 3, Figure 5A).

ChIP assays performed in primary MKs from healthy donors demonstrated that RUNX1 could bind the new region at 2 sites in the MYL9 promoter and at 1 of the 2 binding sites in the MYH9 promoter (MYH9_B; Figure 5B). To test for functional relevance, we cloned wild-type (WT) promoter regions (plucMYL9 and plucMYH9) or promoter regions containing mutation in the RUNX1 binding sites (plucMYL9mut1, mut2, and mut1/2 or plucMYH9mut1, supplemental Table 3) upstream of the luciferase gene and we performed gene reporter assays in the HEL cell line. We found that overexpression of wt RUNX1 with its cofactor CBF β increased luciferase activity in transient transfection assays for both promoter constructs (plucMYL9 and plucMYH9). When the 2 RUNX1 binding sites in the MYL9 promoter region were mutated, a significant decrease in luciferase activity was observed ($n = 2$ in triplicate, $P < .05$; Figure 5C). Similarly, mutation in the RUNX1 binding site B in MYH9 promoter, which was immunoprecipitated in ChIP experiment, also led to a significant decrease in luciferase activity ($n = 2$ in triplicate, $P < .05$; Figure 5C). Together these results demonstrate functional relevance of the identified RUNX1 binding sites.

Inhibition of myosin II activity in FPD/AML rescues the MK ploidization defect

Recently we reported that MYH10, but not MYH9, was involved in MK ploidization and these results were strengthened by the fact that blebbistatin increased the ploidy level in myh9 KO mice.²² To understand whether MYH10 persistence in FPD/AML MK could affect the ploidization process, cultured MKs from 2 patients in each pedigree were treated with 25 μ M blebbistatin. As shown in Figure 6, blebbistatin treatment led to an important increase in ploidy level in all patients MKs and also in control MKs. In pedigree A, the ploidy level increased from 2.8N and 2.9N to 5N and 6.9N, respectively (Figure 6A). In pedigree B, the ploidy increased from 2.2N and 2.6N to 6 and 7.3N, respectively (Figure 6B) and finally, in pedigree D, the ploidy increased from 2.6N and 2.8N to 6.1N and 4.5N, respectively (Figure 6C; $n = 6$ for patient MKs without blebbistatin [$2.65 \pm 0.1N$] and with blebbistatin [$5.96 \pm 0.43N$], $P < .0001$). This result suggests that the sustained MYH10 expression is involved in the decreased ploidy level of MKs from FPD/AML patients.

Discussion

The mechanisms by which RUNX1 mutations contribute to induction of thrombocytopenia in FPD/AML are not completely understood. Only a few studies on platelets from FPD/AML patients have been performed, which have implicated the abnormal expression of genes, such as MPL,¹² MYL9, ALOX12, and TUBB1 and 2¹¹ and others, some of them being directly regulated by RUNX1. However, studies on platelets may not be sufficient to determine the precise mechanisms of the thrombocytopenia because genetic alterations in transcription factors lead to dysmegakaryopoiesis with only a fraction of MKs giving rise to platelets. For this reason, we examined some aspects of the in vitro megakaryopoiesis of 3 FPD/AML pedigrees with different RUNX1 mutations.^{5,12}

We show that the in vitro FPD/AML megakaryopoiesis presented 4 abnormalities. First, peripheral blood CD34⁺ cells yielded

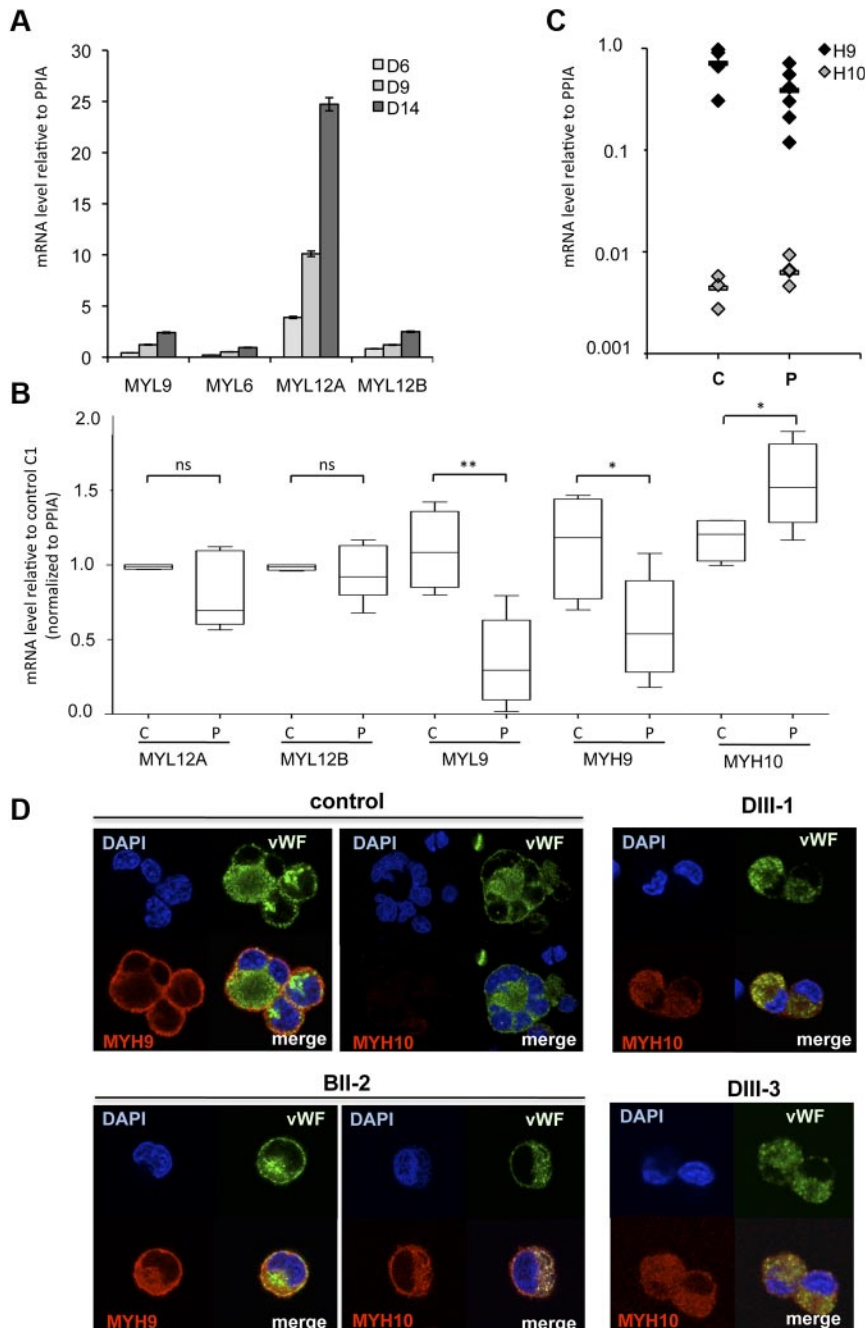


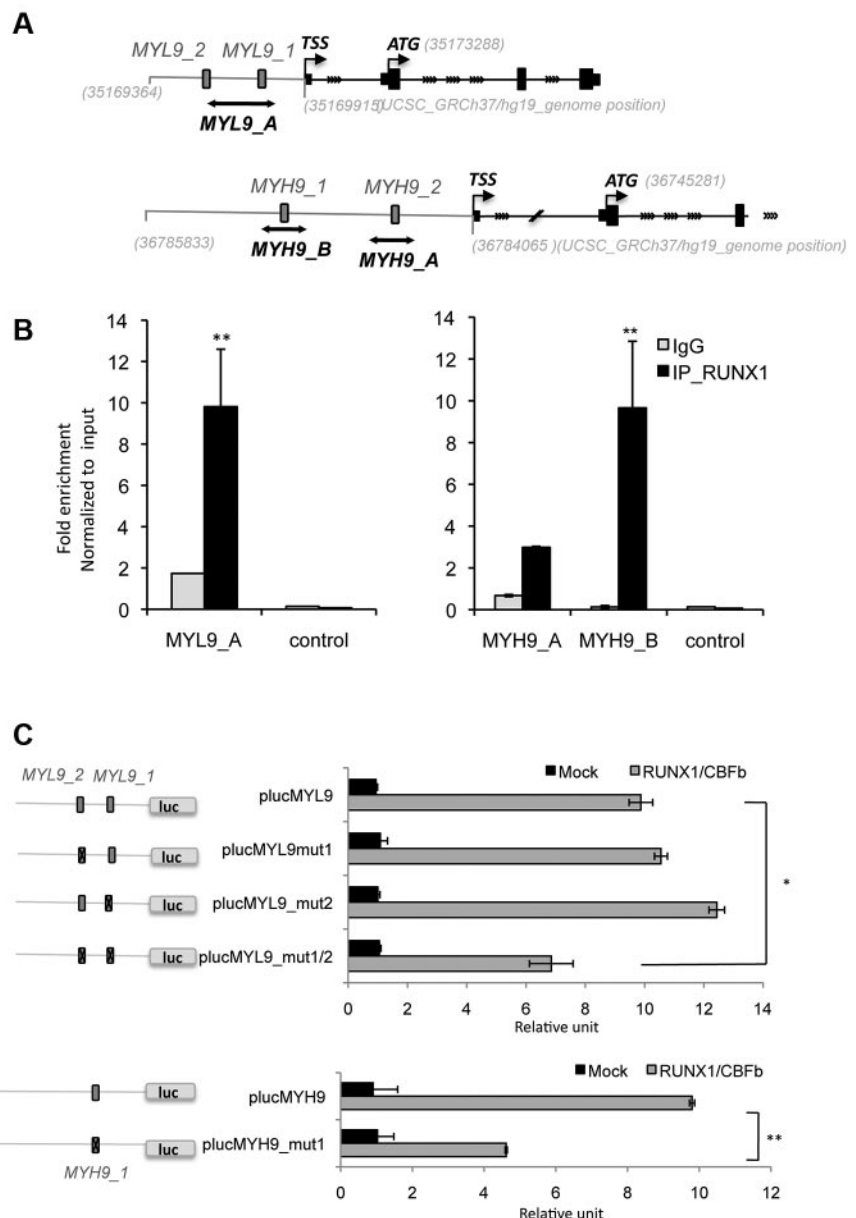
Figure 4. Myosin expression during normal and pathologic MK differentiation. (A) CD41⁺ MKs were derived from adult blood CD34⁺ cells and studied at 3 different days (D6 to D14 corresponding to cells with increasing maturity). MYL9, MYL6, MYL12A and MYL12B mRNA level were determined by real time RT-PCR. The histograms show 1 representative experiment of 2, each in triplicate. Error bars represent \pm SD of triplicate. (B) Expression analysis of MYH9, MYH10, MYL9, MYL12A, and MYL12B genes in MKs of FPD/AML patients. CD34⁺ cells isolated from peripheral blood of 6 patients (P: All-1, All-2, BII-2, BII-3, DIII-1, and DIII-3) and 4 healthy individuals (C) were grown in liquid medium in presence of TPO, IL3, IL6, SCF, and FLT3-L. At day 10 of culture, mature (CD41⁺CD42⁺) MKs were sorted and mRNA level was analyzed by real time RT-PCR. Expression was compared with control C1. (* $P < .05$, ** $P < .01$, \pm SEM 2-tailed welch corrected). (C) MYH9 and MYH10 mRNA levels were detected by real time RT-PCR. (A-C) Real time RT-PCR was normalized to PPIA and HPRT. As similar results were obtained, only results normalized to PPIA are shown. (D) MYH9 and MYH10 proteins were detected by immunofluorescence labeling using antibodies against human MYH10, MYH9 (red), and von Willebrand Factor (VWF, green). Nucleus was stained with DAPI (blue).

a decreased number of MKs. This result is in line with 2 previous reports showing a decreased number of MK progenitors⁹ in the bone marrow in 2 different pedigrees and of MKs in 2 of 5 patients of the same pedigree.³⁰ Second, a marked defect in MK maturation was present as illustrated by a decreased percentage of mature MK (CD41^{high}CD42^{high}) in all the patients whatever the mutation. Third, for the first time, a decrease in the ploidy level of CD34⁺ derived MKs and the presence of microMKs in bone marrow was observed in FPD/AML patients, consistent with the presence of microMKs in the *runx1* KO mouse bone marrow.^{6,22} Finally, mature MKs sorted on the high expression of CD41 and CD42 had a marked defect in proplatelet formation. Thus, FPD/AML thrombocytopenia is the result of a defect at both early and late stages of MK differentiation.

To explain, at least partially, the mechanisms by which RUNX1 deregulates megakaryopoiesis, we focused on actin-myosin com-

plex, which is involved in cytokinesis, migration, adhesion, and proplatelet formation. Recently it was shown that 2 nonmuscle myosin chains, MYL9 and MYH10 are directly regulated by RUNX1,^{21,22} and thus deregulation of their expression could be involved in the dysmegakaryopoiesis in FPD/AML. Nonmuscle myosin II is an actin-binding protein composed of a pair of MHC (myosin heavy chain) and 2 pairs of MLC (myosin light chains). Three isoforms have been characterized with different heavy chains encoded by 3 different genes *MYH9*, *MYH10*, and *MYH14*. Until recently it was considered that MYH9 was the only non-muscle myosin II expressed in the megakaryocytic lineage because it is the only form present in platelets. Recently we reported that MYH10, but not MYH14, is also well expressed in immature MKs and its expression, opposite to MYH9, decreases during megakaryopoiesis to be absent in platelets.²²

Figure 5. MYL9 and MYH9 are direct target genes of RUNX1 in MKs. (A) Schematic representation of *MYL9* and *MYH9* promoters. Gray numbers indicate genomic location in UCSC database (GRCh37/hg19). Gray box indicate RUNX1 putative binding sites (MYL9_1, MYL9_2, MYH9_1, MYH9_2) and black lines show MYL9_A, MYH9_A and MYH9_B amplicon fragments studied in ChIP experiment, respectively localized in position: chr20: 35169598-35169802, chr22:36784345-36784527, chr22: 36785559-36785780. TSS indicates transcription start site and ATG translation start site. (B) Quantitative ChIP analysis was performed in MKs. Primers encompassing (MYL9_A, MYH9_A, MYH9_B) or not (control) RUNX1 site were used to amplify input genomic DNA and the DNA precipitated by antibodies against either normal IgG or RUNX1. A genomic region without RUNX1 binding site was used as negative control sequence (control). Values are normalized to input genomic DNA. Values obtained for fold enrichment using MYH10_A and _B were statistically significant as indicated. Data are representative of 3 independent experiments performed in duplicate ($n = 3$, $P < .001$, error bars represent SD of duplicate). (C) MYL9-promoter luciferase assay with mutated RUNX1 binding sites (plucMYL9mut1, plucMYL9mut2, plucMYL9mut1/2) or with WT promoter (plucMYL9) in HEL cells. Luciferase assay was performed by transient HEL cell cotransfection with 500 ng of MPI vector containing RUNX1 WT and pEF6/V5-His-TOPO vector containing CBF β . Luciferase levels are shown as fold change relative to cells transfected with the promoter construct (plucMYL9, plucMYL9mut1, plucMYL9mut2) or plucMYL9mut1/2 alone. The total amount of transfected DNA was kept constant by transfection with an empty vector. (D) Illustrates 1 representative experiment ($n = 3$, $P < .01$, error bars represent SD of triplicate). (E) MYH9-promoter luciferase assay with (plucMYH9mut1) or without mutated RUNX1 binding site (plucMYH9) in HEL cells. (F) Illustrates 1 representative experiment ($n = 3$, $P < .001$, error bars represent SD of triplicate).



MLC include regulatory light chains (RLCs) and essential light chains (ELCs). The myosin II activity is regulated by the phosphorylation of RLCs. Three highly conserved nonmuscle RLCs (MYL12A, MYL12B, and MYL9) associate with MYH9 and MYH10, as well as the ELC MYL6, immortalized mouse embryo fibroblast NIH 3T3 cell line.³¹ Here we showed that MYL9, MYL12A, MYL12B, and MYL6 are expressed in control MKs and that their expression increases along differentiation with MYL12A being expressed at the highest level. In FPD/AML MKs, expression of only 2 heavy chains, MYH9 and MYH10, and 1 MLC (MYL9) is deregulated.

During polyploidization, MYH10 expression is repressed by RUNX1 and MYH10 down-regulation is necessary for the switch from mitosis to endomitosis.²² In FPD/AML mature MKs we detected a defect in MK polyploidization associated with the persistence of MYH10, which was also detected in circulating platelets.³² This absence of MYH10 silencing may play a role in the defect in MK polyploidization in FPD/AML as attested by its correction by the myosin II chemical inhibitor blebbistatin. The

fact that blebbistatin rescued the ploidization defect in FPD/AML patient suggests that, despite the P19^{INK4D} down-regulation, there is no major additional defect other than myosin deregulation to control DNA replication or the mitotic process.

Expression of MYL9 known to be a RUNX1 target is quasi abolished in MKs from FPD/AML patients. By an in silico approach, we identified 2 regions in the *MYL9* promoter that contained RUNX1 binding sites, one of them being already described.²¹ Both are functional and are occupied by RUNX1 in primary MKs demonstrating the direct involvement of RUNX1 in the transcriptional regulation of *MYL9* during normal MK differentiation. Although a decrease in *MYL9* mRNA level has been reported in FPD/AML platelets,¹¹ the role of *MYL9* silencing in the mechanism of FPD/AML thrombocytopenia is not totally clear. *MYL9* once phosphorylated enhances the motor activity of MYH9, which plays a central role in platelet formation as attested by the macrothrombocytopenia in the MYH9-related disease.³³ MYL12A that is highly expressed in FPD/AML MKs, could associate with MYH10 and MYH9 but this association was only described in

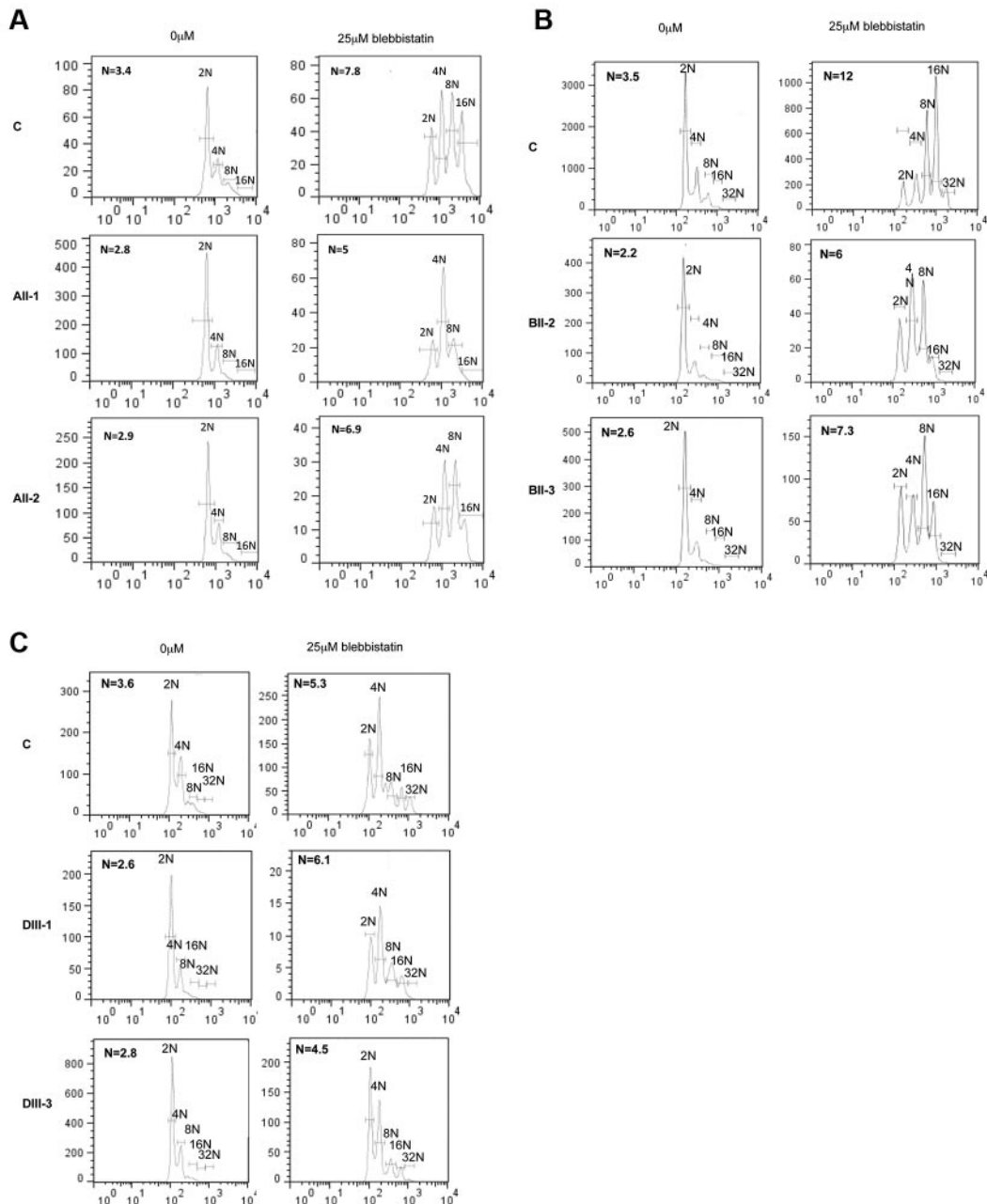


Figure 6. Effect of myosin II activity inhibition on ploidy of FPD/AML MKs. The ploidy level of CD41⁺CD42⁺ MKs was analyzed at day 10 of culture, 72 hours after addition of the myosin II inhibitor, blebbistatin. MK mean ploidy was calculated from the number of cells in each ploidy class. Blebbistatin was used at 25 μ M concentration. The significant increase in ploidy level after addition of blebbistatin was observed in 2 patients of pedigree A (A), 2 patients of pedigree B (B), and 2 patients of pedigree D (C; n = 6, $P < .001$).

fibroblasts,³¹ and it is not known if it occurs in MKs. Previously we have shown that in vitro MYL9 knockdown in primary MKs leads to a defect in proplatelet formation.³⁴ Thus, it is not excluded that the MYL9 preferentially associates with MYH9 during proplatelet formation and that MYH10 has for partners other RLCs during cytokinesis.

Surprisingly MYH9 expression was also approximately 50% decreased in FPD/AML MKs and this was also related to a direct regulation of MYH9 by RUNX1. Indeed 2 functional RUNX1 binding sites were found in the *MYH9* promoter region. The decrease in MYH9 expression after RUNX1 inhibition²² demonstrates that RUNX1 is a transcriptional activator of MYH9, opposite to MYH10 where RUNX1 acts as a repressor. The precise

role of MYH9 in proplatelet formation is controversial. Heterozygous mutations of MYH9 lead to a macrothrombocytopenia in May-Hegglin, Fechtner, Sebastian, and Epstein syndromes,³³ and in heterozygous knock-in mice.³⁵ In contrast the heterozygous *myh9* deletion leading to a true haploinsufficiency does not induce any phenotype in the mouse,³⁶ whereas a complete KO induces a macrothrombocytopenia.²⁷ Discrepant results were also obtained when studies were performed on proplatelet formation. When MKs from *myh9* KO mice were cultured in liquid medium, an increased proplatelet formation was observed,³⁷ whereas in the context of their native environment, a profound decrease in the proplatelet MK number was seen.²⁸ Here we evidenced a decrease of both MYL9 and MYH9 in FPD/AML MKs, which may explain the

defect in proplatelet formation. A concomitant decrease of both myosins leading to a deep defect in actin-myosin complex might explain the absence of macrothrombocytopenia compared with the MYH9 syndrome where a defect in MYH9 alone is present. Moreover, other genes directly or indirectly regulated by RUNX1 could be involved in the defect of proplatelet formation such as TUBB1. In addition, this defect in both tubulin and acto-myosin may explain the presence of unfragmented proplatelets in patient blood as a consequence of a defect in abscission and in the transition from proplatelets to platelets.³⁸

In conclusion, RUNX1-mediated deregulation of MHC and MLC in FPD/AML plays a major role in the mechanism of thrombocytopenia, a finding that emphasizes the role of RUNX1 in the transcriptional regulation of genes implicated in controlling MK and platelet cytoskeleton.

Acknowledgments

The authors thank the patients and their families for participation in this study, Dr Comte (Bastia) and Miss Cadic (Pasteur Cerba laboratory). The authors are grateful to F. Molinas for support and helpful discussion, to F. Wendling for helpful suggestions on the manuscript, to Genethon (Evry, France) for sinpRRL-PGK-GFP lentivirus vector.

This work was supported by grants from the Agence Nationale de la Recherche (ANR-physiopathology, ANR-jeunes chercheurs),

the Ligue contre le Cancer (équipe labellisée 2009), and the Center de Référence des pathologies plaquettaires. D.B. was supported by a postdoctoral fellowship from ANR and L.G. was partially supported by ARC. R.F. and H.R. are recipients of a research fellowship from AP-HP-Inserm (contrat d'interface 2009-2012 for RF and 2008-2013 for HR).

Authorship

Contribution: D.B. designed and performed experiments, analyzed data, and wrote the paper; A.C.G., A.R., N.B., and L.G., performed experiments; P.R., N.D., and P.N. performed experiments and analyzed data; M.C.A. clinical and biologic follow-up of patients; W.V. designed the work, discussed the results, and wrote the paper; P.G.H. performed experiments, discussed results, and wrote the paper; R.F. performed the clinical and biologic follow-up of patients, performed and supervised experiments, and discussed the results; and H.R. designed the work, performed and supervised experiments, and wrote the paper.

Conflict-of-interest disclosure: The authors declare no competing financial interests.

Correspondence: Hana Raslova Inserm UMR1009, Institut Gustave Roussy, 114 rue Edouard Vaillant, 94805, Villejuif cedex, France; e-mail: hraslova@igr.fr.

References

- Preudhomme C, Renneville A, Bourdon V, et al. High frequency of RUNX1 biallelic alteration in acute myeloid leukemia secondary to familial platelet disorder. *Blood*. 2009;113(22):5583-5587.
- Uchida H, Zhang J, Nimer SD. AML1A and AML1B can transactivate the human IL-3 promoter. *J Immunol*. 1997;158(5):2251-2258.
- Taniuchi I, Osato M, Egawa T, et al. Differential requirements for Runx proteins in CD4 repression and epigenetic silencing during T lymphocyte development. *Cell*. 2002;111(5):621-633.
- Okuda T, van Deursen J, Hiebert SW, Grosfeld G, Downing JR. AML1, the target of multiple chromosomal translocations in human leukemia, is essential for normal fetal liver hematopoiesis. *Cell*. 1996;84(2):321-330.
- Bluteau D, Gilles L, Hilpert M, et al. Downregulation of the RUNX1-target gene NR4A3 contributes to hematopoiesis deregulation in familial platelet disorder/acute myelogenous leukemia. *Blood*. 2011;118(24):6310-6320.
- Ichikawa M, Asai T, Saito T, et al. AML-1 is required for megakaryocytic maturation and lymphocytic differentiation, but not for maintenance of hematopoietic stem cells in adult hematopoiesis. *Nat Med*. 2004;10(3):299-304.
- Growney JD, Shigematsu H, Li Z, et al. Loss of Runx1 perturbs adult hematopoiesis and is associated with a myeloproliferative phenotype. *Blood*. 2005;106(2):494-504.
- Putz G, Rosner A, Nuesslein I, Schmitz N, Buchholz F. AML1 deletion in adult mice causes splenomegaly and lymphomas. *Oncogene*. 2006;25(6):929-939.
- Song WJ, Sullivan MG, Legare RD, et al. Haploinsufficiency of CBFA2 causes familial thrombocytopenia with propensity to develop acute myelogenous leukaemia. *Nat Genet*. 1999;23(2):166-175.
- Michaud J, Simpson KM, Escher R, et al. Integrative analysis of RUNX1 downstream pathways and target genes. *BMC Genomics*. 2008;9:363.
- Sun L, Gorospe JR, Hoffman EP, Rao AK. Decreased platelet expression of myosin regulatory light chain polypeptide (MYL9) and other genes with platelet dysfunction and CBFA2/RUNX1 mutation: insights from platelet expression profiling. *J Thromb Haemost*. 2007;5(1):146-154.
- Heller PG, Glembofsky AC, Gandhi MJ, et al. Low Mpl receptor expression in a pedigree with familial platelet disorder with predisposition to acute myelogenous leukemia and a novel AML1 mutation. *Blood*. 2005;105(12):4664-4670.
- Tiedt R, Coers J, Ziegler S, et al. Pronounced thrombocytosis in transgenic mice expressing reduced levels of Mpl in platelets and terminally differentiated megakaryocytes. *Blood*. 2009;113(8):1768-1777.
- Gilles L, Guieze R, Bluteau D, et al. P19INK4D links endomitotic arrest and megakaryocyte maturation and is regulated by AML-1. *Blood*. 2008;111(8):4081-4091.
- Lambert MP, Rauova L, Bailey M, Sola-Visner MC, Kowalska MA, Poncz M. Platelet factor 4 is a negative autocrine in vivo regulator of megakaryopoiesis: clinical and therapeutic implications. *Blood*. 2007;110(4):1153-1160.
- Aneja K, Jalagadugula G, Mao G, Singh A, Rao AK. Mechanism of platelet factor 4 (PF4) deficiency with RUNX1 haploinsufficiency: RUNX1 is a transcriptional regulator of PF4. *J Thromb Haemost*. 2011;9(2):383-391.
- Elagib KE, Racke FK, Mogass M, Khetawat R, Delehanly LL, Goldfarb AN. RUNX1 and GATA-1 coexpression and cooperation in megakaryocytic differentiation. *Blood*. 2003;101(11):4333-4341.
- Kaur G, Jalagadugula G, Mao G, Rao AK. RUNX1/core binding factor A2 regulates platelet 12-lipoxygenase gene (ALOX12): studies in human RUNX1 haploinsufficiency. *Blood*. 2010;115(15):3128-3135.
- Nyby MD, Sasaki M, Ideguchi Y, et al. Platelet lipoxygenase inhibitors attenuate thrombin- and thromboxane mimetic-induced intracellular calcium mobilization and platelet aggregation. *J Pharmacol Exp Ther*. 1996;278(2):503-509.
- Kato H, Ikeda H, Murohara T, Haramaki N, Ito H, Imaizumi T. Platelet-derived 12-hydroxyoctadecatrienoic acid plays an important role in mediating canine coronary thrombosis by regulating platelet glycoprotein IIb/IIIa activation. *Circulation*. 1998;98(25):2891-2898.
- Jalagadugula G, Mao G, Kaur G, Goldfinger LE, Dhanasekaran DN, Rao AK. Regulation of platelet myosin light chain (MYL9) by RUNX1: implications for thrombocytopenia and platelet dysfunction in RUNX1 haploinsufficiency. *Blood*. 2010;116(26):6037-6045.
- Lordier L, Bluteau D, Jalil A, et al. RUNX1-induced silencing of nonmuscle myosin heavy chain IIB contributes to megakaryocyte polyploidization. *Nat Commun*. 2012;3:717.
- Choi ES, Nichol JL, Hokom MM, Hornkohl AC, Hunt P. Platelets generated in vitro from proplatelet-displaying human megakaryocytes are functional. *Blood*. 1995;85(2):402-413.
- Debili N, Masse JM, Katz A, Guichard J, Breton-Gorius J, Vainchenker W. Effects of the recombinant hematopoietic growth factors interleukin-3, interleukin-6, stem cell factor, and leukemia inhibitory factor on the megakaryocytic differentiation of CD34+ cells. *Blood*. 1993;82(1):84-95.
- Lordier L, Chang Y, Jalil A, et al. Aurora B is dispensable for megakaryocyte polyploidization, but contributes to the endomitotic process. *Blood*. 2010;116(13):2345-2355.
- Nurden P, Debili N, Vainchenker W, et al. Impaired megakaryocytopoiesis in type 2B von Willebrand disease with severe thrombocytopenia. *Blood*. 2006;108(8):2587-2595.
- Léon C, Eckly A, Hechler B, et al. Megakaryocyte-restricted MYH9 inactivation dramatically affects hemostasis while preserving platelet aggregation and secretion. *Blood*. 2007;110(9):3183-3191.

28. Eckly A, Rinckel JY, Laeuffer P, et al. Proplatelet formation deficit and megakaryocyte death contribute to thrombocytopenia in Myh9 knockout mice. *J Thromb Haemost*. 2010;8(10):2243-2251.
29. Marinescu VD, Kohane IS, Riva A. MAPPER: a search engine for the computational identification of putative transcription factor binding sites in multiple genomes. *BMC Bioinformatics*. 2005;6:79.
30. Downton SB, Beardsley D, Jamison D, Blattner S, Li FP. Studies of a familial platelet disorder. *Blood*. 1985;65(3):557-563.
31. Park I, Han C, Jin S, et al. Myosin regulatory light chains are required to maintain the stability of myosin II and cellular integrity. *Biochem J*. 2011;434(1):171-180.
32. Antony-Debre I, Bluteau D, Itzykson R, et al. MYH10 protein expression as a biomarker of RUNX1 and FLI1 alterations [published online ahead of print June 7, 2012]. *Blood*. doi: 10.1182/blood-2012-04-422352.
33. Seri M, Cusano R, Gangarossa S, et al. Mutations in MYH9 result in the May-Hegglin anomaly, and Fechtner and Sebastian syndromes. The May-Hegglin/Fechtner Syndrome Consortium. *Nat Genet*. 2000;26(1):103-105.
34. Gilles L, Bluteau D, Boukour S, et al. MAL/SRF complex is involved in platelet formation and megakaryocyte migration by regulating MYL9 (MLC2) and MMP9. *Blood*. 2009;114(19):4221-4232.
35. Zhang Y, Conti MA, Malide D, et al. Mouse models of MYH9-related disease: mutations in non-muscle myosin II-A. *Blood*. 2012;119(1):238-250.
36. Matsushita T, Hayashi H, Kunishima S, et al. Targeted disruption of mouse ortholog of the human MYH9 responsible for macrothrombocytopenia with different organ involvement: hematologic, nephrologic, and otologic studies of heterozygous KO mice. *Biochem Biophys Res Commun*. 2004;325(4):1163-1171.
37. Eckly A, Strassel C, Freund M, et al. Abnormal megakaryocyte morphology and proplatelet formation in mice with megakaryocyte-restricted MYH9 inactivation. *Blood*. 2009;113(14):3182-3189.
38. Thon JN, Macleod H, Begonja AJ, et al. Microtubule and cortical forces determine platelet size during vascular platelet production. *Nat Commun*. 2012;3:852.